

## Temperature dependence of the phonon broadening of the Si 2*p* XPS line

P. Unsworth and J. E. Evans

*IRC in Surface Science, University of Liverpool, P.O. Box 147, Liverpool L69 3BX, United Kingdom*

P. Weightman

*IRC in Surface Science and Department of Physics, University of Liverpool, P.O. Box 147, Liverpool L69 3BX, United Kingdom*

A. Takahashi

*Surface Treatment Research Laboratory, Nippon Steel Corporation, 20-1 Shintomi Futtsu, Chiba-Ken 299-12, Japan*

J. A. D. Matthew

*Department of Physics, University of York, Heslington, York YO1 5DD, United Kingdom*

Q. C. Herd

*VSW Instruments Ltd., Link House, Warwick Road South, Old Trafford, Manchester M16 0JR, United Kingdom*

(Received 8 September 1995; revised manuscript received 7 February 1996)

High-resolution silicon 2*p* photoemission measurements have been obtained using a recently designed state of the art high resolution monochromatized Al x-ray source with our enhanced multidetection system. The temperature dependence of the phonon broadening of the Si 2*p* XPS core lines has been investigated. Up to 470 K there is an increase in linewidth with temperature qualitatively consistent with phonon broadening. In the temperature range >470 K there is a decrease in linewidth with increasing temperature possibly due to enhanced core hole screening. The electron-phonon coupling constant *S* for lightly doped Si was estimated to be in the order of 15 for the temperature region showing a phonon broadening, but the linewidth variation does not behave in a manner consistent with conventional theory. [S0163-1829(96)03126-8]

### I. INTRODUCTION

The rapid creation of a core-hole potential during photoemission, Auger emission, or x-ray-absorption processes, gives rise to the generation of both phonons and plasmons. It is well known that the initial vibrational state in a solid is dependent on the temperature distribution of phonon levels and in consequence the phonon broadening contribution to such processes is found to increase with temperature. The vibrational broadening of x-ray photoemission spectroscopy (XPS) core lines has been explained in terms of a model originally developed by Huang and Rhys<sup>1</sup> to understand optical defects in crystals and reapplied to core-level spectroscopy by Parratt.<sup>2</sup> The thermal broadening of the x-ray-absorption spectra of metals was explained by Overhauser<sup>3</sup> by considering the fluctuating Coulomb potential at the core electrons but with only partial success. More recently Hedin and Rosengren<sup>4</sup> who performed ionic pseudopotential rather than bare Coulomb potential theory, were able to explain the phonon broadening of the soft x-ray-absorption spectra (XAS) of Li, Na, K, and Al. Following these early studies further experimental work was carried out by Citrin, Eisenberger, and Hamann<sup>5</sup> on the study of phonon broadening of XPS core lines from the alkali halides. The results are in good agreement with a theoretical model developed by Mahan<sup>6</sup> employing contributions from six phonon modes over the Brillouin zone. Besides electron-phonon coupling an additional source of phonon broadening results from the recoil energy which the photoejected electron imparts to the ion. Recoil phonon broadening is significant for very low *Z*

ions or highly energetic electrons. For Si over the temperature range of the experiments reported here the recoil phonon broadening is estimated to be in the order of ~5% of the combined phonon contribution, within the errors of the experiment.

There have been a number of studies over the last three decades of phonon broadening of the x-ray photoelectron linewidths of metals and of polar-type materials in general,<sup>1-10</sup> but nonpolar insulators and/or semiconductors have received much less attention. Here we examine the phonon broadening of the 2*p* core photoemission peaks in Si.

The vibrational broadening in polar materials has been explained in terms of the large electron-phonon coupling by Mahan.<sup>6</sup> This vibrational broadening is of Gaussian nature<sup>1,2</sup> and the linewidth ( $\Gamma$ ) at (FWHM) takes the form

$$\Gamma = 2.35 \left[ S(\hbar\omega) \coth\left(\frac{\hbar\omega}{2kT}\right) \right]^{1/2}. \quad (1)$$

This analysis assumes sufficient energy is available to excite a large number of phonons producing a Franck-Condon envelope with a Gaussian line-shape function;  $\omega$  represents in the simplest form of the theory the longitudinal optical frequency  $\omega_{LO}$  excited by the creation of the hole, and *S* is the mean number of phonons excited at 0 K. Silicon is a nonpolar material but Eq. (1) will be applicable.

In XPS the lattice is responding to a change of one electron charge at the site, while in XAS, e.g., to an excitonic state, somewhat weaker coupling will occur. An analysis by Matthew<sup>11</sup> using a semiclassical configurational coordinate

approach, from first principles shows the average phonon linewidth contribution to a photoemission core line can be represented by

$$[\Delta E_{\text{PES}}^2]_{\text{AV}} = \hbar \sum_{i=1}^N \frac{(F_i^t)^2}{2\omega_i} \coth\left(\frac{\hbar\omega_i}{2k_B T}\right), \quad (2)$$

where  $(F_i^t)$  represents the generalized force on an unperturbed oscillator coordinate  $Q_i$  and of frequency  $\omega_i$  in a system with  $N$  degrees of freedom. In the case of ionic crystals the generalized force  $(F_i^t)$  is related to the monopole Coulomb forces between the core hole and the ions in the crystal lattice and also the dielectric properties of the material as in the Huang-Rhys model.<sup>1</sup> Equation (2) applies for any electron coupling mechanism.

Steady improvements in instrumental resolution have made it possible to measure photoelectron linewidths with greater accuracy. The performance of aluminum x-ray source monochromators making a Gaussian or skew Gaussian contributions to photoelectron linewidths have normally been of the order 0.4–0.6 eV and attempts to improve the resolution usually lead to a severe loss of sensitivity. In the experiment reported here we used a high flux and well-focused x-ray gun together with an improved analyzer lens configuration-multidetector system. This enabled us to obtain high sensitivity with a monochromator resolution of  $\sim 0.25$  eV.

## II. EXPERIMENT

Monochromatized x-ray photoelectron spectroscopy was performed using a prototype high-performance spectrometer manufactured by VSW Instruments Ltd. with design specification of 0.25 eV resolution. The x-ray source consisted of Al  $K\alpha$  monochromatized x rays with high-flux output when operating with a power consumption of 600 W. The x-ray monochromator was designed using Johann's geometry and employed precision ground quartz crystals cut parallel to the 1010 plane making the ideal Bragg condition for Al  $K\alpha$  radiation. The electron multidetection system comprised a VSW HA150 hemispherical analyzer used in a fixed analyzer transmission mode (FAT) with variable magnification lens and upgraded channelplate detector. The analyzer was operated in its highest-resolution mode, which from a fit of a Gaussian resolution function to a measurement of the Fermi edge of metallic Ag gives an instrumental resolution of  $\sim 0.27$  eV. Fitting the Si  $2p$  XPS linewidth data after allowing for lifetime broadening of 0.075 eV and surface components<sup>12,13</sup> yielded a Gaussian broadening contribution with temperature dependence. This residual broadening may be due mainly to phonon coupling but may also contain a contribution from inhomogeneity in Si environments associated with sample charging. The vacuum system was pumped by a diffusion pump-cold trap configuration producing an ultimate pressure  $5 \times 10^{-9}$  mB. The silicon (111) wafer [ $n$ -type, P-doped resistivity 0.67–1.33  $\Omega\text{cm}$  and P dopant concentration in the order of  $(4.5\text{--}7.5) \times 10^{15}$  atoms  $\text{cm}^{-3}$ ] was mounted so as to allow direct heating by passing a dc current directly through the sample and indirect heating by radiation from a resistively mounted tungsten coil assembled directly under the specimen. The temperature of the Si specimen was measured with a thermocouple taking several read-

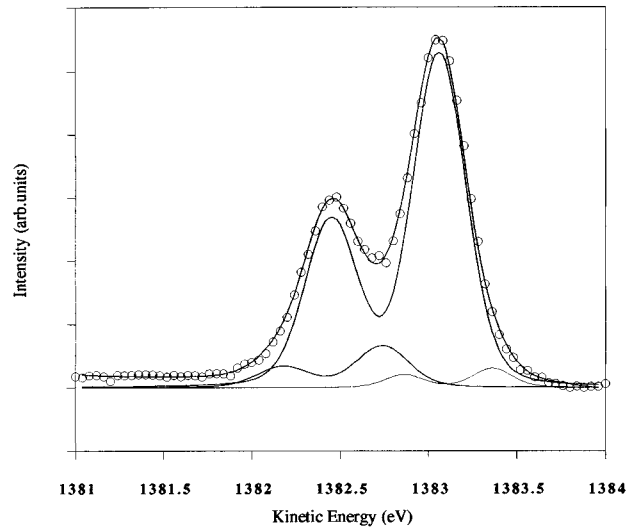


FIG. 1. Silicon  $2p$  spectrum recorded at room temperature. Circles are data points; the solid curves are the fit to the data.

ings in order to find the stabilization point before data acquisition. In order to minimize specimen charging, the sample was earthed at each end during data collection. The Si  $2p$  photoelectron lines were measured at different temperatures up to 773 K. Radiative sample heating during data acquisition did not exceed 1073 K in order to prevent phosphorus surface diffusion and also to prevent the formation of a further Si phase transition from which a  $1 \times 1$  superstructure occurs, yielding an extra surface component<sup>13</sup> in addition to the two which describe the  $7 \times 7$  reconstruction.<sup>14,15</sup> Sample cleaning was achieved by cycles of direct flash heating to 1373 K for short periods with the combination of 2-kV Ar ion sputtering. This procedure was conducted and the surface cleanliness monitored by measurements of the C  $1s$ , O  $1s$  photoelectron lines. After the first flash heating of the specimen a small C  $1s$  photoelectron line was observed, though the O  $1s$  photoelectron line could not be detected. Further heating and sputtering of the sample did not reduce the slight C contamination which, after allowing for the appropriate cross sections<sup>16</sup> and photoelectron escape depths<sup>17</sup> we estimate contributes  $\sim 5\%$  of the total Si  $2p$  signal observed in these experiments.

## III. RESULTS

The spectrum in Fig. 1 shows a clean silicon  $2p$  spectrum and the appropriate line-shape fit recorded at room temperature (RT). The fitting procedure, which includes both bulk and surface components, is described later. The spectrum of Fig. 1 was recorded from just one scan and thus gives some indication of the resolving power and count rate improvements on existing instruments. It is clear that the Si  $2p_{1/2}$  and the  $2p_{3/2}$  are almost completely resolved. Seven Si  $2p$  photoemission spectra are shown in Fig. 2 at temperatures ranging from 315 to 748 K. It can be observed that the magnitude of the dip in intensity between the  $2p_{1/2}$  and the  $2p_{3/2}$  decreases with an increase of temperature indicating an increase in the linewidth of the components. The spectra are plotted with reference to the Fermi edge and a general shift is observed to lower kinetic energy with increasing tempera-

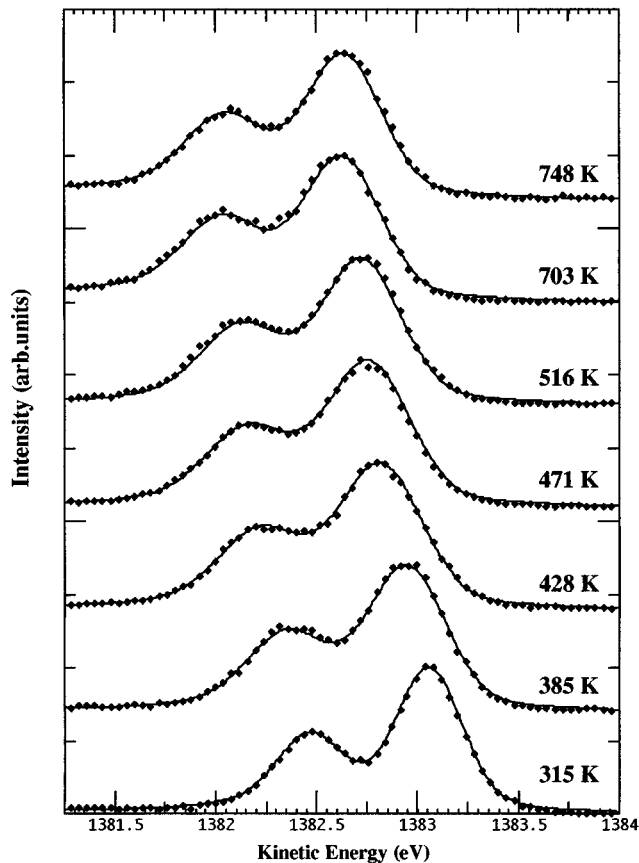


FIG. 2. Silicon  $2p$  data (diamonds) with respective fits (solid lines) shown with increasing temperature.

ture. This shift probably arises from a temperature dependence of the charging of the specimen. A similar effect observed in the XPS spectra of the alkali halides<sup>5</sup> has been related to band-gap effects.

The parametrized fits (shown as continuous lines accompanying each spectrum), were generated by initially representing each component of the spin-orbit doublet by a Lorentzian to allow for lifetime broadening. The spin-orbit splitting was fixed at 0.6 eV and the relative intensity of the main components at 2:1. In each case the fit also included surface components accompanying each core level, with one being shifted to higher kinetic energy by 0.77 eV and the other component shifted to lower kinetic energy by 0.355 eV in agreement with the results of earlier studies.<sup>14,15</sup> The surface components were scaled to optimize the parametrized fits and the Lorentzians were then convoluted with a Gaussian line shape to allow for instrumental and vibrational broadening effects. High-resolution studies using synchrotron radiation to tune the spectrum to the minimum of the photoelectron escape depths have revealed more complicated contributions from surface components.<sup>18–20</sup> Our spectra are dominated by the bulk contributions and the individual surface component intensities had little effect on the results for the temperature dependence of the linewidth.

The only parameter varied in fitting the line shape to the experimental data so as to account for the temperature-dependent broadening was the Gaussian line-shape component. Since lifetime broadening is a constant Lorentzian con-

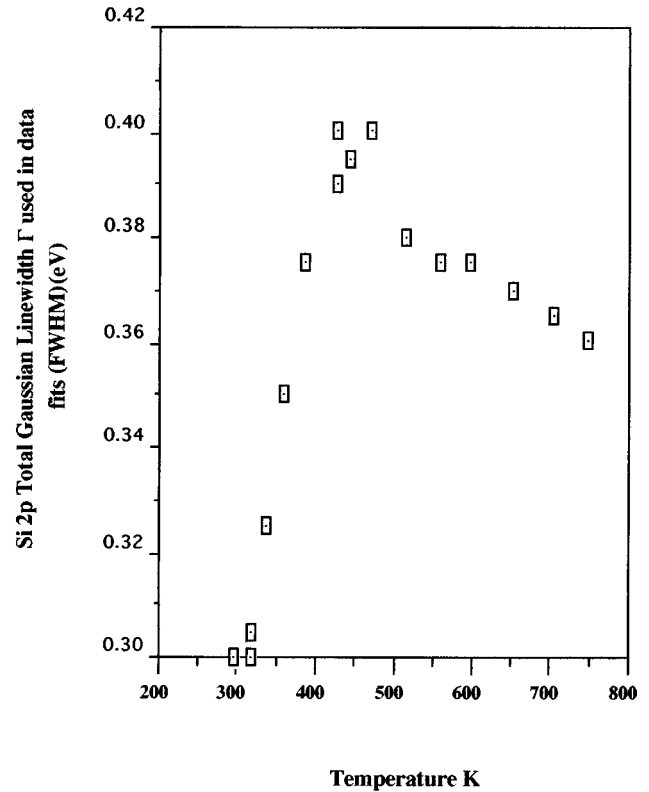


FIG. 3. Plot of Si  $2p$  total Gaussian linewidth contribution (used in each fit) vs temperature K.

tribution of 0.075 eV FWHM and the instrumental contribution assumed Gaussian is also constant at  $\sim 0.27$  eV the difference between the breadth at elevated temperature and room temperature should be associated with the phonon broadening at that temperature and that is assumed in the analysis that follows. Figure 3 shows the change in total Gaussian linewidth (used in the fit) of the Si  $2p$  (eV) versus temperature (K). This Si  $2p$  total Gaussian linewidth shows a linear increase over the range 300–425 K. Beyond the 450-K region the Si  $2p$  total Gaussian linewidth then begins to decrease but at a much slower rate. The total linewidth broadening comprises the phonon broadening contribution and the instrumental broadening added in quadrature ( $\Gamma^2 = \Gamma_{\text{inst}}^2 + \Gamma_{\text{phonon}}^2$ ). This assumes that in this temperature range any broadening due to inhomogeneous charging is included in  $\Gamma_{\text{inst}}^2$ , and that it will not increase with temperature in this temperature range. Figure 4 shows the squared total Gaussian linewidth  $\Gamma^2$  versus  $\coth(\hbar\omega_0/2kT)$ .

#### IV. DISCUSSION

Considerations of phonon coupling in polar materials have provided an understanding of the temperature-dependent linewidths of XPS core line measurements. Citrin *et al.*<sup>5</sup> have measured XPS phonon contributions of the order of 0.7 eV at 300 K, for the  $K(2p_{3/2})$  XPS line in the  $K$  halides. In order for phonon broadening to contribute to XPS linewidths the hole state created initially, must be more tightly coupled to the lattice than the state into which it decays. In consequence the fluctuating potential at the lattice zero point generates phonon broadening from the thermal

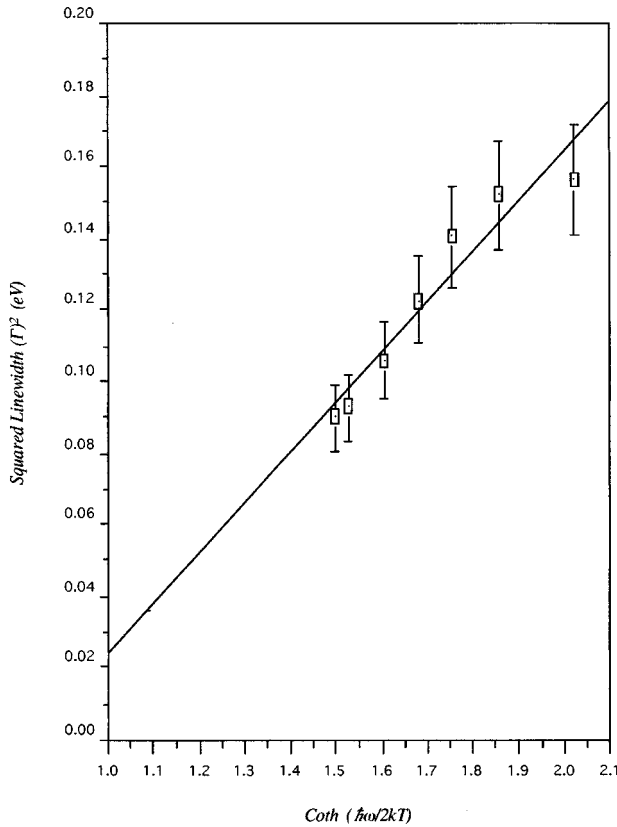


FIG. 4. Graph of squared total Gaussian linewidth  $(\Gamma)^2$  vs  $\coth(\hbar\omega_0/2kT)$ .

excitations of the lattice. This idea is summarized in a simple model due to Citrin and Hamann<sup>21</sup> in which the phonon broadening in XPS is identical in both long and short lifetime limits.

There has been very little work on phonon broadening of XPS core lines in Si except for a room-temperature Si 2*p* measurement by Siegbahn<sup>22</sup> who deduced the phonon broadening of 0.14 eV for silicon (111) at room temperature. A comparable value of phonon linewidth, 0.13 eV, was obtained from our room-temperature results. Phonon broadening observed in the Si 2*p* photoemission of Si(111)-(1×1):H and Si(111)-(1×1):D surfaces has been reported by Karlsson, Owman, Landemark, Chao, Mårtensson, and Uhrberg.<sup>23</sup> Phonon coupling measurements obtained from soft-x-ray emission (SXE) spectroscopy by Carson and Schnatterly<sup>24</sup> on undoped crystalline Si and heavily P-doped ( $n \approx 10^{20} \text{ cm}^{-3}$ ) Si, have provided a determination of the coupling constant  $S$  in Eq. (1). An analysis of the Si  $L_{2,3}$  emission up to 870 K gave a value of the phonon coupling in Si by plotting the  $\sigma^2$  versus  $\coth(\hbar\omega_0/2kT)$ , yielding a line with a gradient  $S(2.35\hbar\omega_0)^2$ . These authors estimated the value of  $\hbar\omega_0$  as 0.04 eV for Si from the atomic mass and bond force constant<sup>25</sup> assuming a breathing mode involving interactions with nearest neighbors only. This value was approximately the longitudinal-acoustical-phonon frequency at the zone boundary. In the case of the heavily P-doped Si, Carson *et al.*<sup>24</sup> found the value of the coupling constant  $S$  to be 0.74. This is much less than that of undoped crystalline Si, a result which Carson *et al.*<sup>24</sup> explained in terms of the increased screening in the P-doped Si. However, in XES the

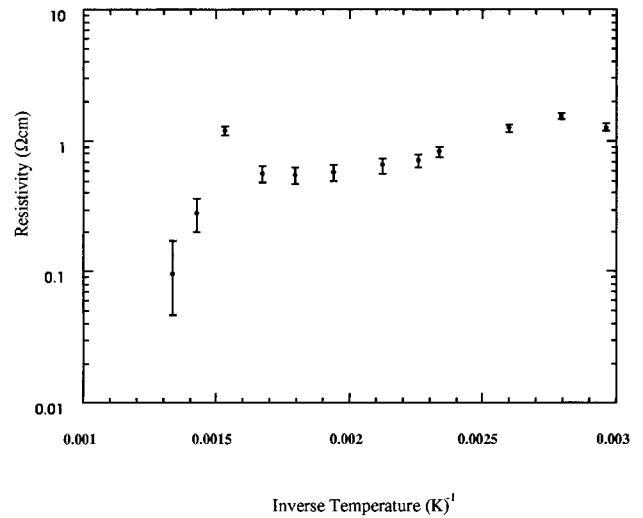


FIG. 5. Silicon resistivity as a function of the inverse temperature.

local charge sensed by the lattice in the initial and final states if very similar, so a smaller  $S$  value than for XPS is expected.

A method, similar to Carson *et al.*<sup>24</sup> of plotting the squared Gaussian linewidth  $\Gamma(\text{FWHM})^2$  versus  $\coth(\hbar\omega_0/2kT)$  was employed on the data; extending the graph back to intersect with the  $Y$  axis yielded a value for  $\Gamma_{\text{inst}}^2 + \Gamma_{\text{phonon}}^2$  (0 K). The intersection point for the extrapolated total Gaussian linewidth  $\Gamma^2$  is less than the expected instrumental width, Fig. 4; even allowing for the large possible error in the intercept; this implies that Eqs. (1) and (2) are not a consistent representation of phonon broadening of the 2*p* core-hole photoemission process in Si. The gradient of the linear region within the graph, Fig. 4, is far less than that obtained for polar materials. The coupling constant  $S$ , estimated by assuming the gradient of the least-squares fit in Fig. 4 to be equal to  $S(2.35\hbar\omega_0)^2$ , was found to be  $\sim 15$  assuming the phonon energy to be in the region of  $\hbar\omega_0 = 0.04$  eV. We find that changing the value of  $\hbar\omega_0$  within a reasonable range in the graph of squared Gaussian linewidth versus  $\coth(\hbar\omega_0/2kT)$  leads only to small changes in gradient. Our result for the value of  $S$  is much larger than that quoted by Carson *et al.*,<sup>24</sup> as expected; the potential changes by one unit of electric charge between the initial and final states in XPS while in the x-ray-absorption process there is less charge at the site. The value of the phonon coupling constants for photoemission in metals usually ranges between 4 and 15, which is comparable to our result for Si in the linear temperature region suggesting a near metallic response to the core hole. The  $S$  value derived from the gradient is, however, inconsistent with the extrapolated value of  $\Gamma^2$  at 0 K. The metals electron-phonon scattering increases with increase of temperature which causes a decrease in relaxation time and hence an increase in electrical resistance. In the case of  $n$ -doped silicon, electron-phonon scattering also increases with increase of temperature but an opposing process of electron excitation across the band gap into the conduction band causes the resistance to decrease due to enhanced carrier concentration. A graph of log resistivity against  $1/T$  for our specimen (Fig. 5) is in excellent agreement with the earlier results for phosphorus-doped Si of

Pearson and Bardeen.<sup>26</sup> At high temperatures the enhanced carrier concentration might imply better screening giving a smaller generalized force on the oscillators of the system following core hole removal and hence reduce phonon broadening. However, the breadth reduction observed could have subtler origins, for example, improved screening may modify the charging pattern in the material leading to greater homogeneity. This would suggest that part of the broadening ascribed to phonons in the lower-temperature region may be associated with different charging environments in the surface region. In the high-temperature region where we observe a reduction in the Si  $2p$  linewidth Pearson and Bardeen<sup>26</sup> conclude that the material is behaving intrinsically with approximately equal concentration of electrons and holes.

### V. CONCLUSION

We have shown that measurements of narrow  $2p$  core lines as in this case Si can be measured with the aid of

high-resolution XPS to exploit phonon contributions in non-lifetime effects of measured linewidths. Phonon broadening of short-lifetime XPS core lines in semiconductors is still in its infancy and therefore in order to understand the effects at higher temperatures  $>RT$  much greater theoretical understanding is required. The coupling constant  $S$  for Si in the temperature region, i.e., RT to 470 K was estimated to have an upper value of  $\sim 15$  from the breadth temperature variations, but this value was not consistent with the extrapolated 0-K breadth. The results suggest that additional mechanisms associated with differential charging are playing a role.

### ACKNOWLEDGMENTS

The participants from Liverpool University and Nippon Steel would like to thank V.S.W. for the use of the prototype high-resolution spectrometer performing this experiment.

- 
- <sup>1</sup>K. Huang and A. Rhys, Proc. R. Soc. A **204**, 406 (1950).  
<sup>2</sup>L. G. Parret, Rev. Mod. Phys. **31**, 616 (1959).  
<sup>3</sup>A. W. Overhauser, Rev. Mod. Phys. **31**, 616 (1959), footnote 108.  
<sup>4</sup>L. Hedin and A. Rosengren, J. Phys. F **7**, 1339 (1977).  
<sup>5</sup>P. H. Citrin, P. Eisenberger, and D. R. Hamann, Phys. Rev. Lett. **33**, 965 (1974).  
<sup>6</sup>G. D. Mahan, Phys. Rev. B **21**, 4791 (1980).  
<sup>7</sup>W. Goldammer, W. Ludwig, W. Zierau, and C. Falter, Surf. Sci. **141**, 139 (1984).  
<sup>8</sup>R. Zimmerman, Appl. Phys. **3**, 235 (1974).  
<sup>9</sup>S. E. Tullinger and S. L. Cunningham, Phys. Rev. B **18**, 1898 (1976).  
<sup>10</sup>P. H. Citrin, G. K. Wertheim, and Y. Baer, Phys. Rev. B **16**, 4256 (1977).  
<sup>11</sup>J. A. D. Matthew, Phys. Rev. B **29**, 3031 (1984).  
<sup>12</sup>R. D. Bringans, M. A. Olmstead, R. I. G. Uhrberg, and R. Z. Bachrach, Phys. Rev. B **36**, 9569 (1987).  
<sup>13</sup>K. Hricovini, G. LeLay, M. Abraham, and J. E. Bonnet, Phys. Rev. B **41**, 1258 (1990).  
<sup>14</sup>T. Miller, T. C. Hsieh, and T.-C. Chiang, Phys. Rev. B **33**, 6983 (1986).  
<sup>15</sup>D. H. Rich, T. Miller, and T.-C. Chiang, Phys. Rev. B **37**, 3124 (1988).  
<sup>16</sup>J. H. Scofield, J. Elec. Spec. Rel. Phen. **8**, 129 (1976).  
<sup>17</sup>D. R. Penn, J. Elec. Spec. Rel. Phen. **9**, 29 (1976).  
<sup>18</sup>J. J. Paggel, W. Theis, K. Horn, Ch. Jung, C. Hellwig, and H. Petersen, Phys. Rev. B **50**, 18 686 (1994).  
<sup>19</sup>G. LeLay, M. Göthelid, T. M. Grehk, M. Björkquist, U. O. Karlsson, and V. Yu. Aristov, Phys. Rev. B **50**, 14 277 (1994).  
<sup>20</sup>C. J. Karlsson, E. Landemark, Y.-C. Chao, and R. I. G. Uhrberg, Phys. Rev. B **50**, 5767 (1994).  
<sup>21</sup>P. H. Citrin and D. R. Hamann, Phys. Rev. B **15**, 2923 (1977).  
<sup>22</sup>K. Siegbahn, Philos. Trans. R. Soc. London A **318**, 3 (1986).  
<sup>23</sup>C. J. Karlsson, F. Owman, E. Landemark, Y.-C. Chao, P. Mårtensson, and R. I. G. Uhrberg, Phys. Rev. Lett. **72**, 4145 (1994).  
<sup>24</sup>R. D. Carson and S. E. Schnatterly, Phys. Rev. B **39**, 1659 (1989).  
<sup>25</sup>W. A. Harrison, *Electronic Structure and the Properties of Solids* (Freeman, San Francisco, 1980), p. 196.  
<sup>26</sup>G. L. Pearson and J. Bardeen, Phys. Rev. **75**, 865 (1949).